Chemistry & Biology
Article

Juxtaposition of Chemical and Mutation-Induced Developmental Defects in Zebrafish Reveal a Copper-Chelating Activity for Kalihinol F

Imelda T. Sandoval,[1,3] Elizabeth J. Manos,[1,3] Ryan M. Van Wagoner,[2] Richard Glenn C. Delacruz,[4] Kornelia Edes,[1,3] Dennis R. Winge,[4] Chris M. Ireland,[2] and David A. Jones[1,2,3,*]
[1]Department of Oncological Sciences
[2]Department of Medicinal Chemistry
University of Utah, Salt Lake City, UT 84112, USA
[3]Huntsman Cancer Institute, 2000 Circle of Hope, Salt Lake City, UT 84112, USA
[4]Departments of Medicine and Biochemistry, University of Utah Health Sciences Center, Salt Lake City, UT 84132, USA
*Correspondence: david.jones@hci.utah.edu
http://dx.doi.org/10.1016/j.chembiol.2013.05.008

SUMMARY

A major hurdle in using complex systems for drug screening is the difficulty of defining the mechanistic targets of small molecules. The zebrafish provides an excellent model system for juxtaposing developmental phenotypes with mechanism discovery using organism genetics. We carried out a phenotype-based screen of uncharacterized small molecules in zebrafish that produced a variety of chemically induced phenotypes with potential genetic parallels. Specifically, kalihinol F caused an undulated notochord, defects in pigment formation, hematopoiesis, and neural development. These phenotypes were strikingly similar to the zebrafish mutant, *calamity*, an established model of copper deficiency. Further studies into the mechanism of action of kalihinol F revealed a copper-chelating activity. Our data support this mechanism of action for kalihinol F and the utility of zebrafish as an effective system for identifying therapeutic and target pathways.

INTRODUCTION

A major challenge in the drug discovery process often centers on assigning in vivo activity to candidate compounds. As a potential solution, zebrafish have proven useful for determining both genetic and molecular mechanisms and may offer a powerful tool for understanding drug mechanisms (Kaufman et al., 2009; Taylor et al., 2010; Zon and Peterson, 2005). Small embryo size and high fecundity of adult females make zebrafish amenable to moderate throughput screening and enable screens that directly affect a specific phenotype. Rapid zebrafish development that occurs ex utero, combined with optical transparency of the embryos, allow for convenient observation of morphologic changes with a dissecting microscope without sacrificing the embryo (Kimmel et al., 1995). Small molecule screening in a whole organism also provides a physiologic context that is lacking in cell-based and in vitro assays and affords preliminary toxicity, tissue specificity, and pharmacokinetic profiles that greatly facilitate lead compound identification and optimization. Most importantly, the zebrafish is a vertebrate system that shares a high degree of genetic and physiologic similarity to humans. Numerous zebrafish genetic mutants have been established that faithfully phenocopy human disease mechanisms and zebrafish-based chemical genetic screens are currently underway to identify compounds that modify disease phenotypes, an approach that promotes development of novel biologic tools and therapeutics (Ingham, 2009; Kaufman et al., 2009; Lieschke and Currie, 2007; MacRae and Peterson, 2003; Shin and Fishman, 2002; Taylor et al., 2010; Zon and Peterson, 2005).

Previous efforts have clearly demonstrated the utility of zebrafish in identifying compounds that affect specific developmental phenotypes. In 2000, Peterson and colleagues carried out one of the earliest zebrafish-based chemical screens and discovered small molecules that perturb normal development of the CNS, cardiovascular system, pigmentation, and ear (Peterson et al., 2000). Since then, numerous screens have revealed chemical modifiers of zebrafish embryonic development (Kaufman et al., 2009; Taylor et al., 2010). However, another approach may exist to use zebrafish to define mechanisms of uncharacterized compounds and compound collections. For example, the kalihinol family of compounds are isonitrile diterpenoids originally isolated from the marine sponge *Acanthella* sp. (Patra et al., 1984). These compounds are characterized by a biflorane carbon skeleton and show a variety of biologic activities that include antibacterial, antifungal, antiparasitic, antifouling, and cytotoxicity against tumor cells (Alvi et al., 1991; Chang et al., 1984; Fusetani et al., 1990; Hirota et al., 1996; Miyaoka et al., 1998; Omar et al., 1988; Sun et al., 2009; Wolf and Schmitz, 1998). Although specific kalihinols, such as kalihinol F, have proposed mechanisms in bacteria and starfish, it is not clear how kalihinols might function within a vertebrate system both from physiologic and mechanistic points of view (Bugni et al., 2004; Ohta et al., 2003).

In this study, we performed a zebrafish-based phenotypic screen of 954 diverse compounds and juxtaposed the observed chemically induced phenotypes with known genetic mutations. This analysis led us to focus on kalihinol F, which produced a

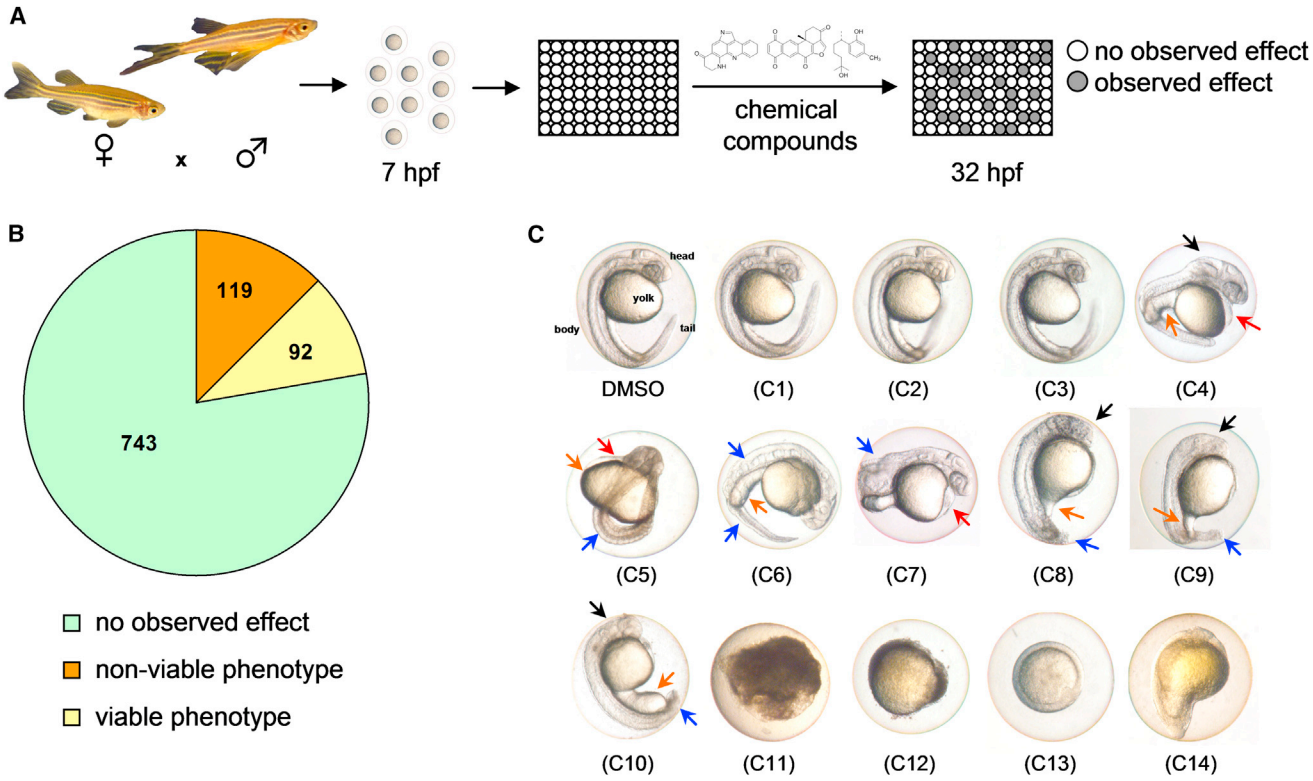

Figure 1. Zebrafish-Based Chemical Screen Leads to Identification of Interesting Phenotypes

(A) Schematic of the zebrafish phenotype screen. Wild-type embryos were arrayed in 96-well plates and treated with 10 μM or 25 μg/ml of test compounds at 7 hpf. Phenotypes were scored at 32 hpf.

(B) Pie chart showing phenotype distribution from the zebrafish screen.

(C) At 32 hpf, zebrafish embryos have a defined head, body, and tail, with a prominent yolk (C, DMSO). Normal-looking embryos were observed for 743 compounds (C1–C3), 119 were toxic to embryos (C11–14), and 92 had viable phenotypes (C4–C10) that include edema (red arrow), underdeveloped head (black arrow), yolk (orange arrow), and tail/body (blue arrow) malformations.

wavy notochord, loss of pigmentation, as well as hematologic and neurologic abnormalities. The kalihinol F-induced phenotypes were highly similar to those reported for the zebrafish mutant *calamity* (*cal*), which shows evidence of copper deficiency due to a mutation in the copper transporter, *atp7a* (Mendelsohn et al., 2006). Consistent with reduced copper levels, kalihinol F-induced phenotypes were prevented with exogenous copper. Further studies demonstrate that kalihinol F chelates copper, an activity shared by other kalihinol analogs. Overall, our findings support this mechanism of action for kalihinol F and demonstrate the use of zebrafish as an effective system for integrating biologic activity with mechanism of action.

RESULTS

A Zebrafish-Based Phenotypic Screen Identifies a Small Molecule Inducing a Copper-Deficient Phenotype

We utilized wild-type zebrafish embryos to screen for bioactive small molecules. For our phenotypic assay, we arrayed 7 hr post-fertilization (hpf) embryos in 96-well plates at one embryo per well, treated with test compounds and visually evaluated developmental phenotypes at 32 hpf (Figure 1A). A total of 954 compounds from different chemical libraries were used in the screen and included synthetic drug-like compounds, US Food and Drug Administration-approved drugs, and natural products (Figure 1B). No discernible effect was observed for the majority of the compounds, resulting in normal-appearing embryos with well-defined body structures at 32 hpf (Figures 1B and 1C, dimethyl sulfoxide [DMSO], c1–c3). Of the active compounds, 119 caused overt lethality (Figures 1B and 1C, c11–c14) while 92 had viable phenotypes that showed varying developmental defects (Figures 1B and 1C, c4–c10). A systematic search of phenotypes elicited by our compound collection against known zebrafish genetic mutants resulted in an interesting match with the zebrafish mutant *calamity* (*cal*). The *calamity* mutant carries a mutation in the ubiquitous copper transporter gene *atp7a* and displays copper deficiency-induced developmental defects (Mendelsohn et al., 2006). Kalihinol F-treated embryos caused defects consistent with copper deficiency (Figures 2B–2D).

Kalihinol F (Figure 2A) is a marine natural product that has been reported to have antibiotic and cytotoxic activities (Alvi et al., 1991; Bugni et al., 2004; Chang et al., 1984; Fusetani et al., 1990; Hirota et al., 1996; Miyaoka et al., 1998; Ohta et al., 2003; Omar et al., 1988; Sun et al., 2009; Wolf and Schmitz, 1998). It has not, however, been associated with copper homeostasis. At 32 hpf, embryos treated with 2.5 μg/ml kalihinol F had an undulated notochord, as confirmed by in situ staining for *ntl*, and a complete absence of pigmentation (Figures 2B–2D). In situ

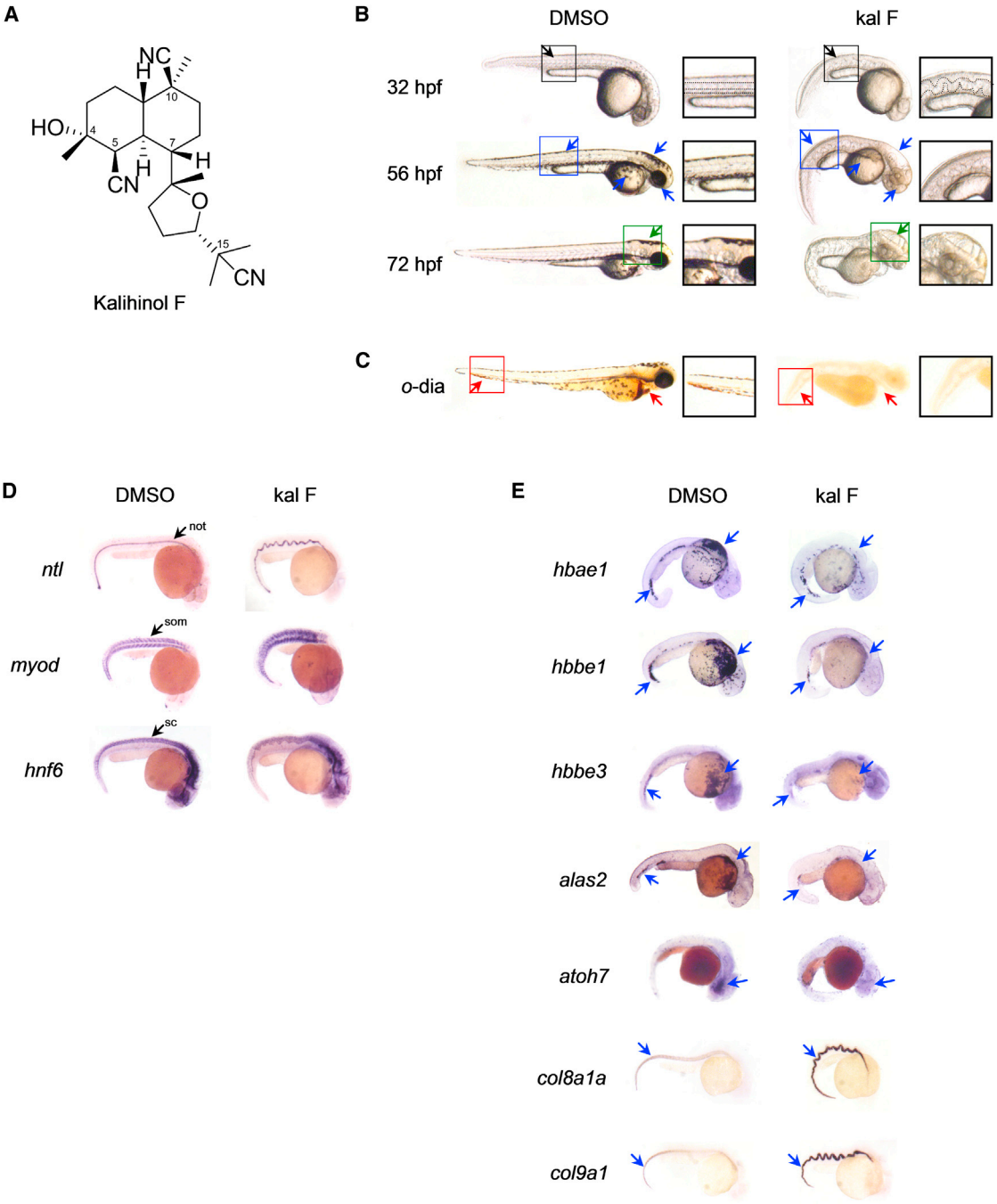

Figure 2. Embryos Treated with Kalihinol F Show a Phenotype Consistent with Copper Deficiency

(A) Chemical structure of kalihinol F.

(B) Exposure of zebrafish embryos to 2.5 μg/ml of kalihinol F (kal F) resulted in a wavy notochord (black arrow, D, ntl), loss of pigmentation (blue arrow) and enlarged hindbrain vesicle (green arrow) as compared to DMSO-treated control embryos. Boxed figures are enlargements of highlighted portions on whole embryos.

(C) *o*-dianisidine staining at 72 hpf revealed loss of hematopoiesis (red arrows) in treated embryos versus control.

(D) In situ hybridization on 32 hpf embryos for *ntl*, *myod*, and *hnf6*. not, notochord; som, somites; and sc, spinal cord.

(E) In situ hybridization for *hbae1*, *hbbe1*, *hbbe3*, *alas2*, *atoh7*, *col8a1a*, and *col9a1* confirms gene expression analysis by RNA sequencing that is consistent with copper-deficient phenotype of kalihinol F.

See also Tables S1 and S2.

Table 1. GO Analysis of the Differentially Regulated Genes in Kalihinol F-Treated Embryos

GO Category	Total Genes	Changed Genes	Enrichment	FDR
Hemoglobin complex	15	8	51.6	0
Oxygen transport	27	8	28.7	0
Oxygen binding	40	9	21.8	0
Heme binding	156	13	8.1	0
Extracellular region	1,430	47	3.2	0
Response to mineralocorticoid stimulus	31	5	15.6	0.001
Inflammatory response	254	12	4.6	0.002
Response to chemical stimulus	2,073	40	1.9	0.006
Organic ether metabolic process	96	7	7.1	0.007
Notochord development	45	5	10.7	0.007
Fibronectin binding	11	3	26.4	0.011
Immune response	548	16	2.8	0.011
Response to progesterone stimulus	31	4	12.5	0.018
Ossification	165	8	4.7	0.020
Regulation of angiogenesis	91	6	6.4	0.020
Lipoprotein metabolic process	96	6	6.0	0.025
Eukaryotic cell surface binding	15	3	19.3	0.025
Triglyceride metabolic process	66	5	7.3	0.031
Vesicle lumen	38	4	10.2	0.032
Protein activation cascade	40	4	9.7	0.035
Cartilage development	151	7	4.5	0.043
Protein maturation	111	6	5.2	0.043
Response to other organism	401	12	2.9	0.044

staining for *myoD* and *hnf6* also revealed short, deformed somites and wavy spinal cord, respectively (Figure 2D). By 56 hpf, loss of pigmentation was more evident. The embryos also appeared curved and had a slow heart beat with no circulation (Figure 2B). The phenotype became progressively worse by 72 hpf, as evidenced by an enlarged hindbrain vesicle, edema, severe body malformation, and crinkly tail (Figure 2B). Loss of blood was confirmed by *o*-dianisidine staining (Figure 2C).

To confirm the bioactivity of kalihinol F at the molecular level, we looked at the gene expression profile of kalihinol F-treated embryos with RNA sequencing. We found that the differentially expressed genes in treated embryos, some of which we confirmed by in situ hybridization, reflected the morphologic defects that we have previously associated with kalihinol F and copper deficiency (Table 1; Figure 2E; Tables S1 and S2 available online). Downregulation was observed for hemoglobin genes such as *hbae1*, *hbbe2*, *hbae3*, *hbbe1*, *hbaa1*, and *hbbe3* that are involved in oxygen transport, heme binding, and formation of the hemoglobin complex. Several genes that are expressed in the brain, eye, and blood were also downregulated. Kalihinol F-treated embryos exhibited increased expression of inflammatory and immune response genes, as well as *col8a1a* and *col9a1*, genes that are both essential for normal notochord and cartilage development and consistent with previous studies reporting elevated collagen levels during copper deficiency (Gansner et al., 2007; Tilton et al., 2006).

Exogenous Copper Prevents Kalihinol F Copper-Deficient Phenotype

Because kalihinol F-treated embryos phenocopy *cal*, we hypothesized that kalihinol F might be inducing copper deficiency either by targeting atp7a, resulting in impaired cellular uptake of copper or by reducing overall levels of bioavailable copper for normal growth and development through copper chelation. To distinguish between the two, treated embryos were given exogenous copper, which will reverse copper chelation but will not overcome defective copper absorption due to inactivated atp7a, as previously shown (Mendelsohn et al., 2006). Exposure of treated embryos to 10 μM $CuCl_2$ led to a complete prevention of the kalihinol F phenotype (93%, n = 120). The notochord appeared normal, as did the somites and spinal cord (Figures 3A and 3B). Normal pigmentation returned and healthy blood circulation was observed (Figures 3A and 3B). To evaluate specificity for copper rescue, embryos were also given zinc and calcium, both +2 metals. Neither zinc (100%, n = 82) nor calcium (100%, n = 27) were capable of reverting any of the kalihinol F-induced embryo defects (Figures 3A and 3B; Figure S1).

Kalihinol F Chelates Copper

Based on the phenotype and copper prevention experiments, our data suggest that kalihinol F might act as a copper chelator. To investigate this further, we performed a modified BCA assay to assess the copper-chelating ability of kalihinol F in comparison with several controls. A constant concentration of $CuCl_2$ was mixed with various concentrations of each of kalihinol F, β-aminopropionitrile (β-APN), and the positive controls EDTA and trientine HCl (T-HCl), a copper chelator used in the clinic to treat Wilson disease (Ding et al., 2011). As expected, a decrease in absorbance due to free copper was observed with increasing concentrations of EDTA and T-HCl (Figure 4A). At 2-fold molar excess, copper was almost completely chelated. A similar behavior was displayed by kalihinol F; there was a reduction in absorbance that was concentration-dependent, although not as steep as that seen with EDTA and T-HCl. The lysyl oxidase inhibitor β-APN did not exhibit any copper chelating activity (Figure 4A).

To further validate the mode of action of kalihinol F, we turned to yeast, whose growth in respiratory-selective media is dependent on copper, a cofactor for Cox1 and Cox2, which are essential for respiration (Weintraub and Wharton, 1981). Wild-type yeast cells grown in glycerol-lactate media supplemented with either kalihinol F or with the known copper chelator, bathocuproine disulphonate (BCS), showed a dose-dependent growth inhibition that was rescued with exogenous copper, but not

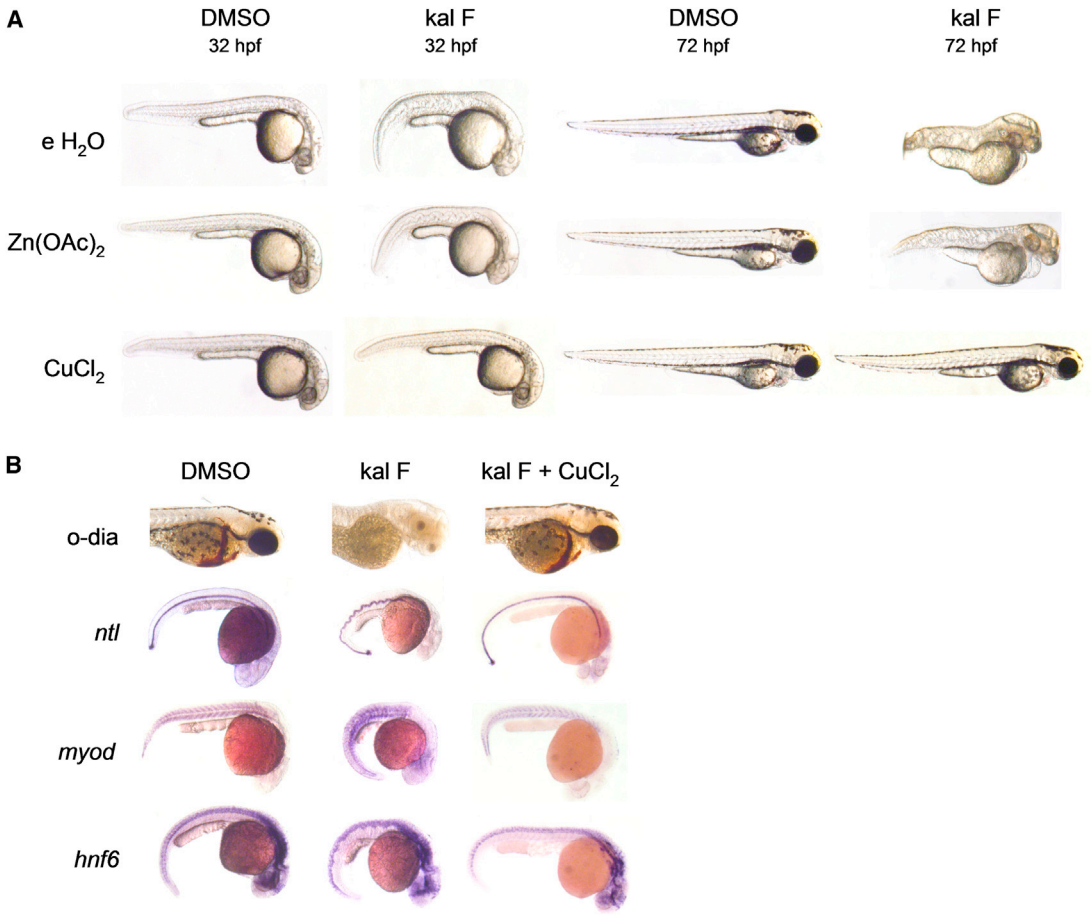

Figure 3. Kalihinol F Phenotype Is Prevented by Addition of Copper

(A) Five hr postfertilization embryos were treated with either DMSO or 2.5 μg/ml kal F then rescued at 7 hpf with 10 μM $CuCl_2$, $Zn(OAc)_2$ and embryo water (e H_2O). Only copper-treated embryos showed normal pigmentation, notochord, and hindbrain comparable to control embryos (bottom row, second and fourth figures from left).

(B) Normal hematopoiesis and rescue of notochord, somites, spinal cord with copper were confirmed by *o*-dianisidine staining and in situ for *ntl*, *myod*, and *hnf6*. See also Figure S1.

iron, which is consistent with the dependency of yeast respiration on copper (Figure 4B).

Because of its paramagnetic nature, copper (II) causes broadening of resonance signals in nuclear magnetic resonance (NMR) spectroscopy as a result of distance-dependent paramagnetic relaxation enhancement (PRE) of nuclear spins (Bloembergen, 1957; Solomon, 1955). To confirm the interactions between kalihinol F and copper by NMR, a titration experiment was performed to measure the effects of addition of $CuCl_2$ on the spectral line widths of kalihinol F in DMSO-d_6. Kalihinol F was present at 11 mM and NMR spectra were collected at the titration end points 0.00, 0.05, 0.10, 0.15, 0.20, 0.30, 0.40, and 0.50 mole equivalents of $CuCl_2$ in D_2O. There was a difference among the signals in the degree of line broadening that occurred in response to copper addition. Some signals exhibited a more rapid onset and more extensive degree of broadening as the titration progressed. The signal for H-5, in particular, was strongly broadened at 0.05 eq Cu (II) and had essentially merged with the baseline by 0.30 eq Cu (II) (Figures 2A and 4C). In addition, the center frequency for H-5 gradually moved upfield as the titration progressed. Before the addition of Cu (II), $\delta_{H\text{-}5}$ occurred at 4.26 ppm. The frequency shifted by 0.03 ppm upfield for each addition of 0.05 eq Cu (II). The remaining signals also exhibited increased broadening as the titration progressed, but did so to a much lesser extent than H-5 (Figure 4C). The remaining signals also displayed smaller shifts in frequency than H-5. Overall, these results suggest that kalihinol F does bind to Cu (II) in DMSO and that the binding site is likely near H-5.

Bioactivity for the Kalihinol Family of Compounds

Kalihinols belong to a large family of multifunctional diterpenes that exhibit a wide array of biologic properties (Alvi et al., 1991; Bugni et al., 2004; Chang et al., 1984; Fusetani et al., 1990; Hirota et al., 1996; Miyaoka et al., 1998; Ohta et al., 2003; Omar et al., 1988; Sun et al., 2009; Wolf and Schmitz, 1998). To investigate whether the copper-chelating activity is shared by other kalihinol analogs, 7 hpf embryos were treated with six additional kalihinol compounds with DMSO as control (Figure 5A). Kalihinol X (100%, n = 50), kalihinol A (99%, n = 75), kalihene (95%, n = 141), and kalihinol G (100%, n = 149) exhibited a similar

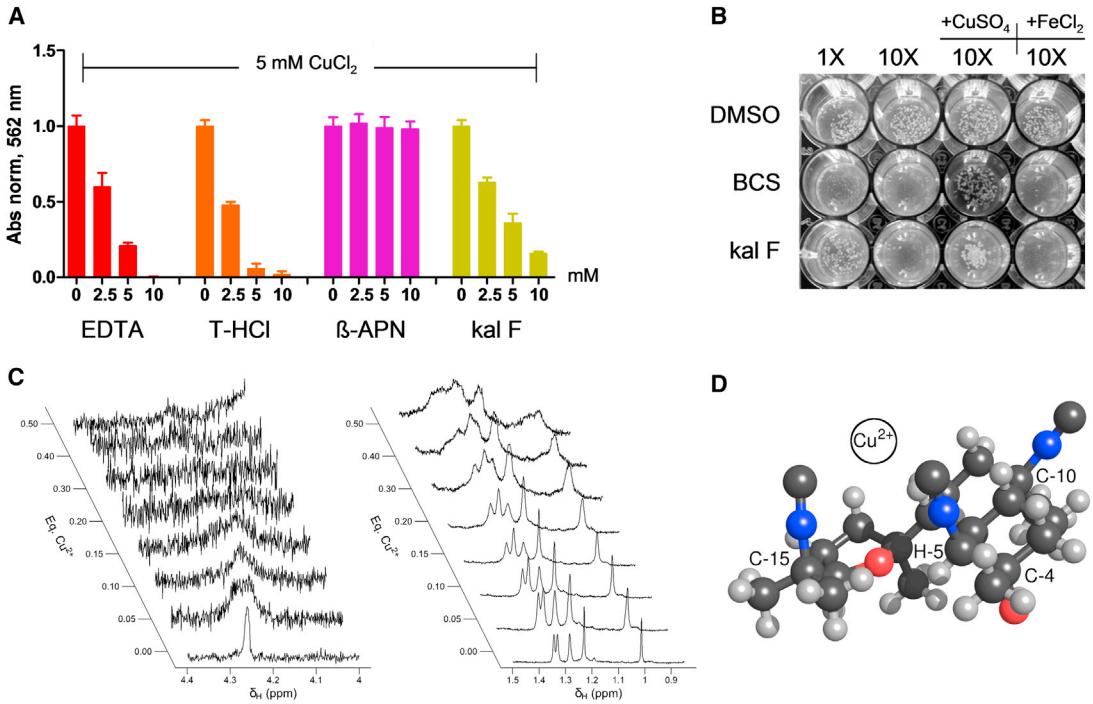

Figure 4. Kalihinol F Is a Copper Chelator

(A) BCA assay was performed on 5 mM $CuCl_2$ supplemented with EDTA, T-HCl, β-APN, or kal F, in increasing molar excess. Copper chelation was determined by measuring absorbance at 562 nm. Graph shown above is representative of multiple experiments. Values indicate mean ± SD.

(B) Wild-type W303 yeast cells were grown on YP-agar plate containing respiration-selective media treated with DMSO, BCS or kal F. Growth inhibition due to limiting copper levels was evaluated visually. Addition of copper, but not iron, was able to rescue yeast growth (lanes 3 and 4). Picture shown above is representative of multiple experiments.

(C) Effects of addition of Cu^{2+} to the ^1H NMR line widths of H-5 (left panel) and the methyl group signals (right panel) of kalihinol F.

(D) Proposed binding site of copper based on previously determined X-ray structure of kalihinol F (Patra et al., 1984). Note that the isonitrile groups attached to C-5 and C-15 are oriented toward the same face of the molecule and potentially forms a bidentate coordination site for Cu^{2+} as depicted. Note also the proximity of H-5 and the furan ether group.

See also Figure S3.

copper-deficient phenotype at 2.5 μg/ml (Figure 5B). Pulcherrimol (95%, n = 107) only showed activity at a higher concentration of 25 μg/ml and this was reflected in the NMR analysis of the interaction between pulcherrimol and copper (Figures 5B and 5C). When a second titration was carried out on a sample containing pulcherrimol, the onset of line broadening was less extensive for pulcherrimol compared to kalihinol F, which suggests a weaker affinity of pulcherrimol for Cu (II) (Figures 4C and 5C). Kalihinol Y (100%, n = 48), was not active at all (Figure 5B). As previously observed with kalihinol F, the copper-deficient phenotype induced by the kalihinol analogs was prevented by treatment with copper (Figure 5B).

Kalihinol F Mitigates Toxicity Associated with Overexposure to Copper

Copper chelation therapy has long been used to treat Wilson disease (WD), a disorder characterized by hepatic accumulation of copper due to mutations in *ATP7b*, a liver-specific copper transporter (Huster, 2010). To determine if kalihinol F can prevent the harmful effects of excess copper, 5 hpf embryos were given 5 μM $CuCl_2$ and were further treated with 5 μg/ml kalihinol F or 10 μM T-HCl. At 72 hpf, embryos exposed to copper remained in their chorion. They appeared shorter and exhibited growth defects that include a pinched yolk extension (96%, n = 142) and a smaller head, as confirmed by in situ for *fabp7* (95%, n = 48, Figure 6A). In situ hybridization for *crx* and *tfa* also revealed smaller eyes (100%, n = 52) and liver (91%, n = 74), respectively (Figure 6A). Treatment with kalihinol F reversed the developmental defects associated with copper toxicity. The rescued embryos were indistinguishable from control embryos with normal yolk extension (100%, n = 102) and well-developed head (100%, n = 42), eyes (100%, n = 50), and liver (91%, n = 55, Figure 6A). Similar results were observed for T-HCl (Figure 6A).

To determine if kalihinol F can overcome the toxic effects of copper in liver cells, human hepatocarcinoma cells (HepG2) were treated with 80 μM $CuCl_2$ and then rescued with 30 μg/ml kalihinol F or 160 μM T-HCl. Quantitative RT-PCR was done to evaluate gene expression changes associated with chemical treatments over 24 hr. Consistent with previous studies by Muller and colleagues, HepG2 cells incubated with copper showed reduced expression of *COMMD1* and *COMMD2* while metallothioneins such as *MT1B*, *MT1E*, *MT1F*, and *MT2A*, along with *HMOX* and heat shock proteins, *HSPA1B* and *HSPCA*, were significantly upregulated (Figure 6B; Muller et al., 2007). Further treatment with either kalihinol F or T-HCl

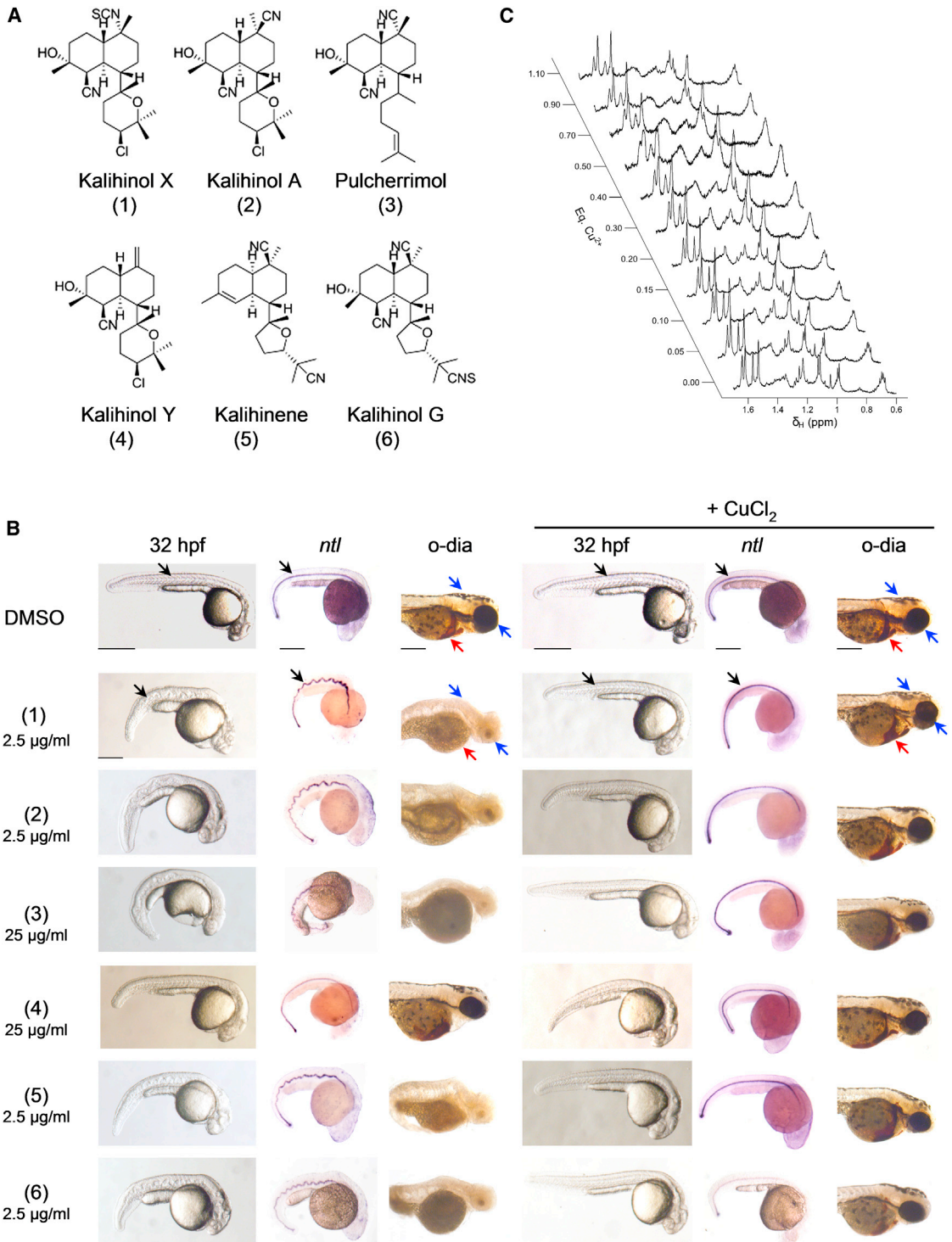

Figure 5. Other Members of the Kalihinol Family also Show Copper Chelating Activity

(A) Chemical structure of kalihinol analogs.

(B) Seven hr postfertilization embryos were treated with either 25 μg/ml or 2.5 μg/ml of kalihinol analogs and DMSO vehicle control (first, second, and third columns). For phenotype rescue experiments, 5 hpf embryos were treated with kalihinols and given $CuCl_2$ at 7 hpf (fourth, fifth, and sixth columns). Embryos were monitored for wavy notochord (black arrow), loss of pigmentation (blue arrow), and hematopoiesis (red arrow).

(C) Effects of addition of Cu^{2+} to the ^{1}H NMR line widths of the methyl signal region of pulcherrimol.

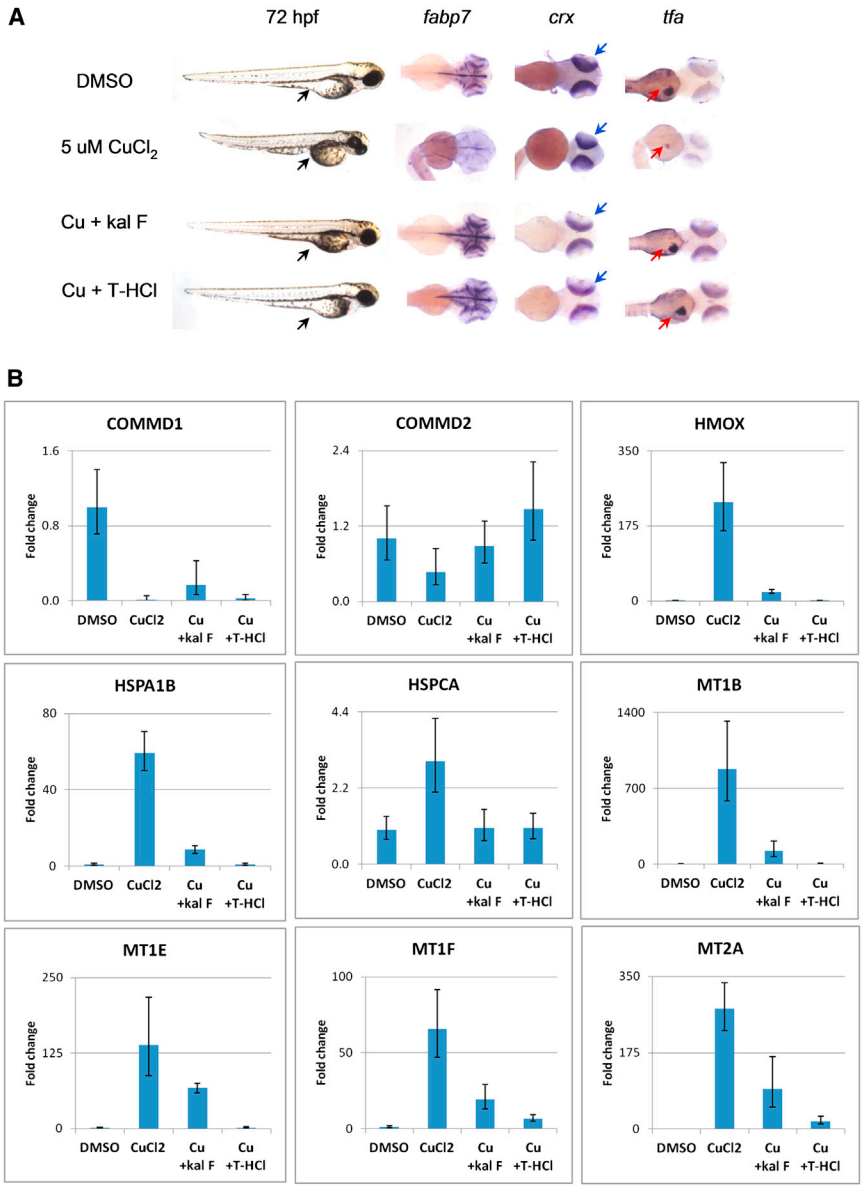

Figure 6. Kalihinol F Reverses Adverse Effects of Copper Toxicity

(A) Five hr postfertilization embryos were treated with 5 μM $CuCl_2$ and rescued at 7 hpf with either 5 μg/ml kalihinol F or 10 μM T-HCl. Excessive copper resulted in a smaller embryo with pinched yolk extension (lane 1, black arrow), small head (lane 2) and eyes (lane 3), and impaired liver development (lane 4). In situ hybridization for *fabp7*, *crx* (blue arrow), and *tfa* (red arrow) revealed normal head development, eye size and proper liver formation, respectively, for embryos rescued with kalihinol F or T-HCl.

(B) Human HepG2 cells were treated with 80 μM copper and rescued with either 30 μg/ml kalihinol F or 160 μM T-HCl. Quantitative RT-PCR showed gene expression changes induced by copper were reversed by either kalihinol F (Cu + kal F) or T-HCl (Cu + T-HCl). Graph shown above is representative of at least two experiments. Values represent mean ± SD.

See also Figure S2 and Table S3.

reversed these trends, although the effect seen with T-HCl is more pronounced compared with kalihinol F (Figure 6B). This could be due to a lower amount of kalihinol F (30 μg/ml ~78 μM) given to cells because of a limited supply of the compound. There also was toxicity in HepG2 cells exposed to copper, as evidenced by floating debris, which was alleviated in rescued cells (Figure S2).

DISCUSSION

Defining the bioactivity and mechanism of action of small molecules is often a challenge in the development of potential therapeutics. We have demonstrated that chemical screening in zebrafish, coupled with genetic analyses, allows for the evaluation of the biologic effects of active compounds with better insight into their molecular mechanism. Our data revealed kalihinol F to be a copper chelator, which evoked developmental abnormalities similar to the known copper transport mutant, *calamity (cal)* (Mendelsohn et al., 2006).

Prior work on kalihinols has been limited to understanding their bioactivity in non-vertebrate systems and to date, has not identified a specific molecular mechanism (Alvi et al., 1991; Bugni et al., 2004; Chang et al., 1984; Fusetani et al., 1990; Hirota et al., 1996; Miyaoka et al., 1998; Ohta et al., 2003; Omar et al., 1988; Sun et al., 2009; Wolf and Schmitz, 1998). Consistent with the phenotype observed for kalihinol F-treated embryos, our BCA assay data indicate that kalihinol F can sequester copper, although not as well as EDTA or T-HCl, a commonly used drug in copper chelation therapy against Wilson disease (Figure 4A; Ding et al., 2011). Kalihinol F exhibited the same activity in yeast, where we exploited the dependency of yeast cells on copper for growth under respiratory-selective media (Figure 4B; Weintraub and Wharton, 1981). Utilizing NMR to detect copper binding with kalihinol F, we found that it displayed a significant affinity for Cu (II) but did not exhibit the tightness of binding seen with β-penicillamine, another clinically used copper chelator (Figure 4C; Figure S3; Ding et al., 2011). Although the affinity of kalihinol F for Cu (II) is weaker, it is predominantly hydrophobic and may offer the advantage of being able to penetrate hydrophobic media and potentially to transport Cu (II) passively through barriers such as cell membranes. Interestingly, both T-HCl and β-penicillamine did not result in any phenotype when given to zebrafish embryos (data not shown).

Based on the previously published X-ray structure of kalihinol F, we propose that copper sits in a binding pocket in the vicinity of H-5, formed by the isonitrile groups on C-5 and C-15 (Figure 4D; Patra et al., 1984). Both H-5 and the tetrahydrofuran

ring are located equatorially on their respective rings and are in proximity to each other. Moreover, the isonitrile groups on C-5 and C-15 are both located on the same face of the ring assembly. The lone-pair electrons on the carbon atoms of these groups are strong candidates for being involved in coordination to Cu (II), suggesting that it might be possible for them to form a bidentate binding site for Cu (II). It is interesting to note, however, that the inactive analog, kalihinol Y, lacks the C-15 isonitrile group, which suggests that the C-5 isonitrile moiety is critical for copper binding (Figures 5A and 5B). This is consistent with the effect of copper on H-5, as seen in our NMR data (Figure 4C).The other isonitrile on C-10 is located equatorially and is, therefore, not capable of intramolecularly coordinating a Cu (II) atom at the proposed binding site (Figure 4). In the X-ray structure of kalihinol F, the isonitrile groups at C-5 and C-15 are roughly parallel to one another and 4.1 Å apart, which would not be a favorable geometry for binding to the same Cu (II) atom. However, a slight rotation around the C-7/C-11 bond and/or the C-14/C-15 bond could yield a more favorable binding site. Such a rotation could also change the magnetic environment near H-5, accounting for the strong perturbation in its chemical shift and its line width.

The differences in the bioactivity of the kalihinol compounds that we additionally screened revealed functionalities that may be important for copper chelation (Figure 5). In comparing the structural differences among the kalihinol analogs, our data indicate the significance of the substituted tetrahydropyranyl/tetrahydrofuranyl moiety and the cyano functional group at C-11 and C-10, respectively. Further studies are needed to examine how the cyano group at C-10 contributes to the overall stability of the copper-kalihinol complex, despite its distance from the proposed binding site on the molecule.

Copper is an essential mineral for normal growth and development of living organisms. It is an important cofactor for a number of metabolic enzymes involved in cellular respiration, energy metabolism, collagen cross-linking, antioxidation, and pigment formation, among others (Tisato et al., 2010). Copper homeostasis is tightly regulated, as evidenced by human ailments resulting from unbalanced copper levels (Tisato et al., 2010). Wilson disease (WD), characterized by copper accumulation in the liver and marked by neurodegenerative symptoms and hepatotoxicity, is a genetic disease caused by mutations in ATP7B, an ATPase copper-transporting enzyme that is primarily responsible for copper elimination in the liver (Huster, 2010). Copper chelation therapy has been a successful treatment strategy for WD, however, the spectrum of chelators available are limited and harbor some toxicities (Ding et al., 2011; Huster, 2010; Tisato et al., 2010; Tümer and Møller, 2010). The ability of kalihinol F to reverse copper toxicity in zebrafish embryos and human HepG2 cells to a similar extent as T-HCl, suggests that kalihinols may have clinical relevance as copper chelators (Figures 6A and 6B).

The copper-chelating activity exhibited by kalihinols is consistent with a large body of literature reporting isonitrile/isocyanide compounds interacting with copper and cuproenzymes (Liu and Reiser, 2011; Reedy et al., 1995; Rhames et al., 2001). One of the most recent is a report by Zhang and colleagues, where they show that an isocyanide antifouling compound, Isocyanide 1, caused a wavy notochord in zebrafish embryos and phenocopied copper deficiency (Zhang et al., 2012). The discovery of kalihinols as copper chelators might aid in identifying potential binding partners responsible for the wide array of biologic activity reported for these compounds.

In conclusion, we used zebrafish to rapidly assign an activity and mechanism of action to kalihinol F. Interestingly, a combined zebrafish-yeast chemical genetic screen undertaken by Ishizaki and colleagues identified 45 compounds affecting copper metabolism in zebrafish embryos that included reported copper chelators and the known MEK inhibitor, U0126, revealing a copper-dependent target pathway for U0126 and further supporting the utility of the zebrafish in elucidating a mechanism of action of small molecules (Ishizaki et al., 2010). The kalihinol family of compounds signifies a class of copper chelators that may be used as a biologic tool to better elucidate the molecular mechanisms underlying copper homeostasis. Kalihinols may represent a copper-chelating pharmacophore. However, to effectively use kalihinols as copper chelators, further studies are required to fully characterize its binding affinity to copper. Kalihinol F may not complex copper as strongly as clinically used copper chelators but preliminary SAR analysis presented in this study can facilitate in developing more potent, kalihinol-based copper chelators that are already membrane permeable and bioavailable.

SIGNIFICANCE

Elucidating the mechanistic action of small molecules is frequently restricted by the complexities of vertebrate model systems. By using an approach of juxtaposing chemically induced phenotypes from our zebrafish screen to known genetic zebrafish mutations, we identified kalihinol F and the kalihinol family as a class of copper chelators. Our findings may lead to the development of more potent copper chelators that may prove useful in the clinic. We have also shown the utility of zebrafish as an effective system for rapidly assigning a mechanism of action to small molecules that may be used to more efficiently identify therapeutic and target pathways.

EXPERIMENTAL PROCEDURES

Zebrafish Maintenance

All animal procedures were approved by the Institutional Animal Care and Use Committee at the University of Utah. Wild-type *Danio rerio* (zebrafish) were maintained as previously described (Westerfield, 1995). Fertilized embryos were collected following natural spawnings either in 1 × E3 medium (286 mg/l NaCl, 13 mg/l KCl, 48 mg/l $CaCl_2 \cdot 2H_2O$, 40 mg/l $MgSO_4$, 0.01% methylene blue) or 2 × PTU (1 × E3 medium, 30.4 mg/l phenylthiourea) and allowed to develop at 28.5°C.

Zebrafish Phenotype Screen and Additional Drug Treatments

Embryos were periodically checked for death and developmental delay before treatment. At 7 hpf, embryos were arrayed in 96-well plates at one embryo/well. Sample compounds were then added to the desired concentration, with DMSO as control. DMSO was kept at 0.5% of the total assay volume.

Embryos were examined visually for viable and nonviable phenotypes with a dissecting microscope at 24 hr posttreatment (hpt). Embryos were photographed live with an Olympus DP71 digital camera. All experiments were repeated at least twice, in duplicate.

Compounds used in the screen were prepared in DMSO either as 10 mM or 5 mg/ml stocks. Further dilutions were carried out in DMSO. The Spectrum Collection library was purchased from MicroSource Discovery Systems

(Gaylordsville, CT). The DIVERSet library was purchased from ChemBridge (San Diego, CA). The chemistry and marine natural product libraries are proprietary to the University of Utah.

For copper prevention experiments, embryos were treated with kalihinol compounds at 5 hpf. Copper chloride ($CuCl_2 \cdot 2H_2O$), calcium chloride ($CaCl_2$) or zinc acetate ($ZnOAc_2$) was added 2 hr later at 5 or 10 μM final concentration, with embryo water as control. Phenotype suppression was evaluated 24 hr after treatment with $CuCl_2$.

For kalihinol rescue experiments, embryos were treated with 5 uM $CuCl_2$ at 5 hpf. Trientine·2HCl (T-HCl) or kalihinol F was added 2 hr later at 10 μM or 5 μg/ml final concentration, with DMSO as control. Phenotype rescue was evaluated 72 hpt with copper chelators.

In Situ Hybridization

In situ hybridizations were performed as previously described using digoxigenin-labeled riboprobes for *ntl* (no tail), *myod* (myogenic differentiation 1), *hnf6* (hepatocyte nuclear factor 6), *hbae1* (hemoglobin alpha embryonic-1), *hbbe1* (hemoglobin beta embryonic-2), *hbbe3* (hemoglobin beta embryonic-3), *alas2* (δ-aminolevulinate synthetase 2), *atoh7* (atonal homolog 7), *col8a1a* (collagen type VIII, alpha 1a), *col9a1* (collagen type IX, alpha 1), *fabp7a* (fatty acid binding protein 7), *crx* (cone-rod homoebox), and *tfa* (transferrin-a) (Nadauld et al., 2004).

o-Dianisidine Staining

o-Dianisidine staining was performed as previously described (Mendelsohn et al., 2006). The embryos were then fixed with 8% paraformaldehyde/2 × sucrose buffer at room temperature for 2 hr or overnight at 4°C.

RNA Sequencing and Data Analyses

RNA was isolated from embryos treated with kalihinol F or DMSO at 32 hpf using the RNeasy kit (QIAGEN). Quadruplicate biologic replica samples were prepared and sequenced using Illumina HiSeq 2000 (Illumina). Raw data were aligned using Novoalign (Novocraft) against the Zv9 genome build containing known and theoretical splice junctions from Ensembl transcript annotation. After converting splice junction matches to genomic coordinates, the OverDispersedRegionScanSeqs (Useq) was used to identify differentially expressed genes using an estimated FDR of 10% and 2-fold difference. GO term analysis was performed using GoMiner (discover.nci.nih.gov/gominer).

BCA Assay

Bicinchoninic acid (BCA) assay was performed according to the manufacturer's instructions with minor modifications (Pierce, Thermo Scientific). EDTA, T-HCl, β-aminopropionitrile (β-APN), or kalihinol F was added to $CuCl_2$ in 0, 0.5, 1, and 2 molar ratios. The resulting solutions were incubated at room temperature for 30 min to allow copper chelation to proceed and then incubated at 37°C for 15 min after the addition of bicinchoninic acid and BSA. Samples were read on the spectrophotometer at 562 nm.

NMR Analysis

NMR experiments were carried out on a Varian INOVA 500 MHz spectrometer with a 3 mm Nalorac MDBG probe. Kalihinol F and pulcherrimol were each dissolved in DMSO-d_6 (240 μl, 11 mM) and were titrated using 26 mM $CuCl_2$ in D_2O. β-penicillamine was dissolved in DMSO-d_6 (240 μl, 18 mM) and was titrated using 48 mM $CuCl_2$ in D_2O. ^1H NMR spectra were recorded after each titration step with mixing at a sample temperature of 298 K. For each spectrum, 16,384 data points were acquired (acquisition time 2.05 s) with a spectral width of 8,000 Hz. Spectra were Fourier-transformed directly with no window functions applied.

Yeast Culture and Drug Treatments

Wild-type W303 yeast cells were cultured in liquid yeast peptone (YP)-glucose at 30°C overnight. Approximately 400 cells were spotted per well in 48-well YP-agar plate prepared with 2%-glycerol-2% lactate as carbon source and supplemented with kalihinol F, bathocuproine disulphonate, or DMSO as control. The culture plate was incubated at 30°C and yeast cell growth inhibition due to chelation of available copper in the media was monitored visually for 2 days. Final drug concentration was either 0.5 or 5 μg/ml for kalihinol F and 0.1 or 1 mM for BCS.

For growth rescue experiments, YP-agar plates were additionally treated with either 50 uM or equimolar copper sulfate ($CuSO_4$) or iron chloride ($FeCl_2$) for kalihinol F- and BCS-containing wells, respectively.

Cell Culture and Drug Treatments

Human hepatocellular carcinoma (HepG2) was obtained from ATCC and was cultured according to the manufacturer's protocols. Cells were plated in six-well plates, seeded at 500,000 cells/well on day 1, and then treated with 80 μM $CuCl_2$ or DMSO the following day. The cells were then rescued with 30 μg/ml kalihinol F or 160 μM T-HCl 1 hr later and incubated at 37°C for 24 hr.

Quantitative RT-PCR

RNA from cell lysates was isolated using the RNeasy kit (QIAGEN). cDNA was synthesized from 4 μg of total RNA using Superscript III (Invitrogen). When possible, intron-spanning primers were designed using the Universal ProbeLibrary Assay Design Center (Roche Applied Science). A complete list of primer sets is provided in Table S3.

PCR master mix was prepared with the LightCycler 480 Probes Master kit and Universal ProbeLibrary probes according to the manufacturer's protocols (Roche Applied Science). PCR was performed in quadruplicate using the LightCycler 480 System (Roche Applied Science) with 45 cycles of amplification and annealing temperature of 60°C. Fold change in gene expression was measured by normalizing against 18S rRNA and comparing compound-treated samples with DMSO-treated control.

SUPPLEMENTAL INFORMATION

Supplemental Information includes three figures and three tables and can be found with this article online at http://dx.doi.org/10.1016/j.chembiol.2013.05.008.

ACKNOWLEDGMENTS

We wish to thank the following: R. Looper and M. Sigman for providing the University of Utah chemistry department chemical library, D. Nix and S. Hammoud for help in analyzing the RNA sequencing data, and HSC core facilities at the University of Utah. This work was supported by an NIH T32 Postdoctoral Training grant (to R.G.C.D. and D.R.W), NIH CA36622 (to C.M.I.), NCI 5PO1CA073992-14 (to D.A.J.), NCI 5RO1CA116468-08 (to D.A.J.), and the Huntsman Cancer Foundation (to D.A.J.). Funding for the NMR spectrometer was provided by NSF grant DBI-0002806 and NIH grants RR06262 and RR14768. The project described was supported by award number P30CA042014 from the National Cancer Institute. The content is solely the responsibility of the authors and does not necessarily represent the official views of the National Cancer Institute or the National Institutes of Health.

I.T.S. and D.A.J. conceived the study design; I.T.S., E.J.M., R.M.V., R.G.C.D., and K.E. performed the experiments; I.T.S., E.J.M., R.M.V., R.G.C.D., D.R.W., C.M.I., and D.A.J. analyzed the data; I.T.S., R.M.V., R.G.C.D., and D.A.J. wrote the paper; all the authors have read, revised, and approved the manuscript.

Received: October 30, 2012
Revised: May 10, 2013
Accepted: May 13, 2013
Published: June 20, 2013

REFERENCES

Alvi, K.A., Tenenbaum, L., and Crews, P. (1991). Anthelmintic polyfunctional nitrogen-containing terpenoids from marine sponges. J. Nat. Prod. *54*, 71–78.

Bloembergen, N. (1957). Proton relaxation times in paramagnetic solutions. J. Chem. Phys. *27*, 572–573.

Bugni, T.S., Singh, M.P., Chen, L., Arias, D.A., Harper, M.K., Greenstein, M., Maiese, W.M., Concepción, G.P., Mangalindan, G.C., and Ireland, C.M. (2004). Kalihinols from two Acanthella cavernosa sponges: Inhibitors of bacterial folate biosynthesis. Tetrahedron *60*, 6981–6988.

Chang, C.W.J., Patra, A., Roll, D.M., Scheuer, P.J., Matsumoto, G.K., and Clardy, J. (1984). Kalihinol-A, a highly functionalized diisocyano diterpenoid antibiotic from a sponge. J. Am. Chem. Soc. *106*, 4644–4646.

Ding, X., Xie, H., and Kang, Y.J. (2011). The significance of copper chelators in clinical and experimental application. J. Nutr. Biochem. *22*, 301–310.

Fusetani, N., Yasumuro, K., Kawai, H., Natori, T., Brinen, L., and Clardy, J. (1990). Kalihinene and isokalihinol B, cytotoxic diterpene isonitriles from the marine sponge Acanthella klethra. Tetrahedron Lett. *31*, 3599–3602.

Gansner, J.M., Mendelsohn, B.A., Hultman, K.A., Johnson, S.L., and Gitlin, J.D. (2007). Essential role of lysyl oxidases in notochord development. Dev. Biol. *307*, 202–213.

Hirota, H., Tomono, Y., and Fusetani, N. (1996). Terpenoids with antifouling activity against barnacle larvae from the marine sponge Acanthella cavernosa. Tetrahedron *52*, 2359–2368.

Huster, D. (2010). Wilson disease. Best Pract. Res. Clin. Gastroenterol. *24*, 531–539.

Ingham, P.W. (2009). The power of the zebrafish for disease analysis. Hum. Mol. Genet. *18*(R1), R107–R112.

Ishizaki, H., Spitzer, M., Wildenhain, J., Anastasaki, C., Zeng, Z., Dolma, S., Shaw, M., Madsen, E., Gitlin, J., Marais, R., et al. (2010). Combined zebrafish-yeast chemical-genetic screens reveal gene-copper-nutrition interactions that modulate melanocyte pigmentation. Dis. Model. Mech. *3*, 639–651.

Kaufman, C.K., White, R.M., and Zon, L. (2009). Chemical genetic screening in the zebrafish embryo. Nat. Protoc. *4*, 1422–1432.

Kimmel, C.B., Ballard, W.W., Kimmel, S.R., Ullmann, B., and Schilling, T.F. (1995). Stages of embryonic development of the zebrafish. Dev. Dyn. *203*, 253–310.

Lieschke, G.J., and Currie, P.D. (2007). Animal models of human disease: zebrafish swim into view. Nat. Rev. Genet. *8*, 353–367.

Liu, M., and Reiser, O. (2011). A copper(I) isonitrile complex as a heterogeneous catalyst for azide-alkyne cycloaddition in water. Org. Lett. *13*, 1102–1105.

MacRae, C.A., and Peterson, R.T. (2003). Zebrafish-based small molecule discovery. Chem. Biol. *10*, 901–908.

Mendelsohn, B.A., Yin, C., Johnson, S.L., Wilm, T.P., Solnica-Krezel, L., and Gitlin, J.D. (2006). Atp7a determines a hierarchy of copper metabolism essential for notochord development. Cell Metab. *4*, 155–162.

Miyaoka, H., Shimomura, M., Kimura, H., Yamada, Y., Kim, H.-S., and Yusuke, W. (1998). Antimalarial activity of kalihinol A and new relative diterpenoids from the Okinawan sponge, Acanthella sp. Tetrahedron *54*, 13467–13474.

Muller, P., van Bakel, H., van de Sluis, B., Holstege, F., Wijmenga, C., and Klomp, L.W. (2007). Gene expression profiling of liver cells after copper overload in vivo and in vitro reveals new copper-regulated genes. J. Biol. Inorg. Chem. *12*, 495–507.

Nadauld, L.D., Sandoval, I.T., Chidester, S., Yost, H.J., and Jones, D.A. (2004). Adenomatous polyposis coli control of retinoic acid biosynthesis is critical for zebrafish intestinal development and differentiation. J. Biol. Chem. *279*, 51581–51589.

Ohta, E., Ohta, S., Hongo, T., Hamaguchi, Y., Andoh, T., Shioda, M., and Ikegami, S. (2003). Inhibition of chromosome separation in fertilized starfish eggs by kalihinol F, a topoisomerase I inhibitor obtained from a marine sponge. Biosci. Biotechnol. Biochem. *67*, 2365–2372.

Omar, S., Albert, C., Fanni, T., and Crews, P. (1988). Polyfunctional diterpene isonitriles from marine sponge Acanthella carvenosa. J. Org. Chem. *53*, 5971–5972.

Patra, A., Chang, C.W.J., Scheuer, P.J., Van Duyne, G.D., Matsumoto, G.K., and Clardy, J. (1984). An unprecedented triisocyano diterpenoid antibiotic from a sponge. J. Am. Chem. Soc. *106*, 7981–7983.

Peterson, R.T., Link, B.A., Dowling, J.E., and Schreiber, S.L. (2000). Small molecule developmental screens reveal the logic and timing of vertebrate development. Proc. Natl. Acad. Sci. USA *97*, 12965–12969.

Reedy, B.J., Murthy, N.N., Karlin, K.D., and Blackburn, N.J. (1995). Isocyanides as ligand-directed indicators of cu(I) coordination in copper proteins. Probing the inequivalence of the cu(I) centers in reduced dopamine-beta-monooxygenase. J. Am. Chem. Soc. *117*, 9826–9831.

Rhames, F.C., Murthy, N.N., Karlin, K.D., and Blackburn, N.J. (2001). Isocyanide binding to the copper(I) centers of the catalytic core of peptidylglycine monooxygenase (PHMcc). J. Biol. Inorg. Chem. *6*, 567–577.

Shin, J.T., and Fishman, M.C. (2002). From Zebrafish to human: modular medical models. Annu. Rev. Genomics Hum. Genet. *3*, 311–340.

Solomon, I. (1955). Relaxation processes in a system of two spins. Phys. Rev. *99*, 559.

Sun, J.-Z., Chen, K.-S., Yao, L.G., Liu, H.-L., and Guo, Y.-W. (2009). A new kalihinol diterpene from the Hainan sponge Acanthella sp. Arch. Pharm. Res. *32*, 1581–1584.

Taylor, K.L., Grant, N.J., Temperley, N.D., and Patton, E.E. (2010). Small molecule screening in zebrafish: an in vivo approach to identifying new chemical tools and drug leads. Cell Commun. Signal. *8*, 11.

Tilton, F., La Du, J.K., Vue, M., Alzarban, N., and Tanguay, R.L. (2006). Dithiocarbamates have a common toxic effect on zebrafish body axis formation. Toxicol. Appl. Pharmacol. *216*, 55–68.

Tisato, F., Marzano, C., Porchia, M., Pellei, M., and Santini, C. (2010). Copper in diseases and treatments, and copper-based anticancer strategies. Med. Res. Rev. *30*, 708–749.

Tümer, Z., and Møller, L.B. (2010). Menkes disease. Eur. J. Hum. Genet. *18*, 511–518.

Weintraub, S.T., and Wharton, D.C. (1981). The effects of copper depletion on cytochrome c oxidase. J. Biol. Chem. *256*, 1669–1676.

Westerfield, M. (1995). The Zebrafish Book. A Guide for the Laboratory Use of Zebrafish (Danio rerio), Third Edition, *Volume 385* (Eugene, OR: University of Oregon Press).

Wolf, D., and Schmitz, F.J. (1998). New diterpene isonitriles from the sponge Phakellia pulcherrima. J. Nat. Prod. *61*, 1524–1527.

Zhang, Y.-F., Kitano, Y., Nogata, Y., Zhang, Y., and Qian, P.-Y. (2012). The mode of action of isocyanide in three aquatic organisms, Balanus amphitrite, Bugula neritina and Danio rerio. PLoS ONE *7*, e45442.

Zon, L.I., and Peterson, R.T. (2005). In vivo drug discovery in the zebrafish. Nat. Rev. Drug Discov. *4*, 35–44.